*Anal. Chem.* **2000,** *72,* 276−285

# Combined Scanning Electrochemical−Atomic Force Microscopy

Julie V. Macpherson* and Patrick R. Unwin*

*Department of Chemistry, University of Warwick, Coventry, U.K. CV4 7AL*

**A combined scanning electrochemical microscope (SECM)−atomic force microscope (AFM) is described. The instrument permits the first simultaneous topographical and electrochemical measurements at surfaces, under fluid, with high spatial resolution. Simple probe tips suitable for SECM−AFM, have been fabricated by coating flattened and etched Pt microwires with insulating, electrophoretically deposited paint. The flattened portion of the probe provides a flexible cantilever (force sensor), while the coating insulates the probe such that only the tip end (electrode) is exposed to the solution. The SECM−AFM technique is illustrated with simultaneous electrochemical-probe deflection approach curves, simultaneous topographical and electrochemical imaging studies of track-etched polycarbonate ultrafiltration membranes, and etching studies of crystal surfaces.**

The scanning electrochemical microscope (SECM) is a scanned probe microscope (SPM) that has proven to be a powerful instrument for the quantitative investigation of a wide range of processes that occur at interfaces.[1] The probe tip in SECM is an ultramicroelectrode (UME), which typically has a characteristic dimension in the 0.1−10 $\mu$m range,[2] although smaller electrodes have occasionally been used.[3,4] The amperometric, or potentiometric, response of the tip UME is recorded as the probe is scanned either normal to the interface of interest (tip approach measurements) or over the interface typically at some fixed height (for imaging purposes) or is held in a fixed position with respect to the substrate (for time-dependent measurements). For imaging experiments with amperometric tips, the SECM current response—recorded as a function of tip position—depends on both the substrate topography and reactivity, with a spatial resolution typically governed by the electrode dimensions.[1]

For samples that show variations in both reactivity and topography, it is difficult to resolve these two components with conventional SECM fixed height measurements. In this situation, a second electroactive mediator is usually added to the solution to provide information on the topography of the sample.[1e,5,6] Moreover, in high-resolution imaging experiments, which require small tips and close electrode−substrate separations, tip crash and resulting sample damage is more likely with fixed height amperometric imaging. A major challenge in SECM is thus to develop new strategies for determining sample topography and reactivity independently.[7−11] For imaging the redox activity of interfaces, vertical tip position modulation has been shown to be a useful approach for distinguishing between contrasting conducting and inert sites.[7,8] An alternative nonelectrochemical technique for maintaining a constant tip−substrate separation has also been introduced.[10,11] By measuring the shear force damping of the UME, dithered laterally at resonant frequency—an approach similar to that used to regulate the substrate−probe separation in scanning near-field optical microscopy (SNOM)[12]—it is possible to map sample topography, independent of the amperometric measurement, with micrometer and submicrometer vertical resolution.[10,11] However, in these measurements the absolute tip−substrate separation is still unknown.

The atomic force microscope (AFM) maps the topography of a substrate with nanometer vertical resolution, by monitoring the interaction force between the sample and a sharp tip, which is attached to the end of a cantilever.[13] AFM methodology is often used to provide a feedback mechanism for height control in SNOM.[14] In an exciting development, it has been shown that AFM can be combined with scanning ion conductance microscopy

(1) For reviews, see for example: (a) Barker, A. L.; Gonsalves, M.; Macpherson, J. V.; Slevin, C. J.; Unwin, P. R. *Anal. Chim. Acta* **1999**, *385*, 223. (b) Unwin, P. R. *J. Chem. Soc., Faraday Trans.* **1998**, *94*, 3183. (c) Mirkin, M. V. *Anal. Chem.* **1996**, *68*, A177. (d) Bard, A. J.; Fan, F.-R. F.; Mirkin, M. V. In *Electroanalytical Chemistry*; Bard, A. J., Ed.; Marcel Dekker: New York, 1994; Vol. 18, pp 243−373. (e) Bard, A. J.; Fan, F.-R. F.; Pierce, D. T.; Unwin, P. R.; Wipf, D. O.; Zhou, F. *Science* **1991**, *254*, 68.

(2) Wightman, R. M.; Wipf, D. O. In *Electroanalytical Chemistry*; Bard, A. J., Ed.; Marcel Dekker: New York, 1989; Vol. 15.

(3) (a) Fan, F.-R. F.; Bard, A. J. *Science* **1995**, *267*, 871. (b) Fan, F.-R. F.; Kwak, J.; Bard, A. J. *J. Am. Chem. Soc.* **1996**, *118*, 9669.

(4) (a) Zhu, Y. Y.; Williams, D. E. *J. Electrochem. Soc.* **1997**, *144*, L43. (b)-Williams, D. E.; Mohiuddin, T. F.; Zhu, Y. Y. *J. Electrochem. Soc.* **1998**, *145*, 2664.

(5) Lee, C.; Kwak, J.; Bard, A. J. *Proc. Natl. Acad. Sci. U.S.A.* **1990**, *87*, 1740.

(6) (a) Gonsalves, M.; Barker, A. L.; Macpherson, J. V.; Unwin, P. R.; O'Hare, D.; Winlove, C. P., in press. (b) Macpherson, J. V.; O'Hare, D.; Unwin, P. R.; Winlove, C. P. *Biophys. J.* **1997**, *73*, 2771.

(7) Wipf, D. O.; Bard, A. J. *Anal. Chem.* **1992**, *64*, 1362.

(8) Wipf, D. O.; Bard, A. J.; Tallman, D. E. *Anal. Chem.* **1993**, *65*, 1373.

(9) (a) Borgwarth, K.; Ebling, D. G.; Heinze, J. *Ber. Bunsen-Ges. Phys. Chem.* **1994**, *98*, 1317. (b) Borgwarth, K.; Ebling, D. G.; Heinze, J. *Electrochim. Acta.* **1994**, *40*, 1455.

(10) Ludwig, M.; Kranz, C.; Schuhmann, W.; Gaub, H. E. *Rev. Sci. Instrum.* **1995**, *66*, 2857.

(11) James, P. I.; Garfias-Mesias, L. F.; Moyer, P. J.; Smyrl, W. H. *J. Electrochem. Soc.* **1998**, *145*, L64.

(12) (a) Shiku, H.; Dunn, R. C. *Anal. Chem.* **1999**, *71*, A23. (b) Betzig, E.; Finn, P. L.; Weiner, J. S. *Appl. Phys. Letts.* **1992**, *60*, 2484. (c) Toledo-Crow, R.; Yang, P. C.; Chen, Y.; Vaez-Iravani, M. *Appl. Phys. Lett.* **1992**, *60*, 2957.

(13) (a) Binnig, G.; Quate, C. F.; Gerber, Ch. *Phys. Rev. Lett.* **1986**, *56*, 930. (b) Rugar, D.; Hansma, P. K. *Phys. Today* **1990**, *43*, 23. (c) Wiesendanger, R. *Scanning Probe Microscopy and Spectroscopy*; Cambridge University Press: Cambridge, U.K., 1994.



10.1021/ac990921w CCC: $19.00 
Published on Web 12/10/1999

(SICM) to produce a technique capable of acquiring conductivity and topography data, simultaneously.[15] The device employs a bent glass pipet filled with electrolyte solution to function as both a force sensor for AFM imaging and a conductance probe for SICM imaging. With this methodology, the topography of a Nucleopore membrane in solution was imaged while simultaneously detecting the conductivity of individual pores, 200 nm in diameter.[15b] However, in contrast to SECM, SICM monitors the overall ion current and is therefore chemically insensitive toward individual ions and neutral molecules.

There has recently been some progress made toward combining SECM and AFM.[4,16,17] In one approach, a commercial AFM was adapted for use as an SECM.[4] However, simultaneous electrochemical and topographical measurements were not described. Initial studies, from our group, employed Pt-coated AFM tips, insulated at all but the cantilever and the tip, to induce dissolution at a crystal surface electrochemically and, subsequently, to image the evolving topography of the sample in response to the perturbation.[16] Although the topographical measurements were at high resolution, the electrochemical measurement was not spatially sensitive, with an exposed electrode area of 0.5−1.00 mm$^2$. Improvements in the spatial resolution of electrochemical measurements were achieved by imaging hydrated substrates in air using a Pt-coated AFM tip.[17] Simultaneous contact mode images of electrochemical activity and surface topography were made of a track-etched porous membrane, hydrated with a solution containing an electroactive mediator.[17] With only the apex of the Pt-coated tip in contact with the hydrated surface, the active electrode area was drastically reduced to the nanometer scale. Unfortunately, this approach cannot be used for work under solution, which forms the overwhelming majority of applications of SECM.

In this paper, we provide details of the development of a combined SECM−AFM for imaging under fluids, capable of providing simultaneous topographical and electrochemical measurements, with high spatial resolution. The probe, which serves as both a force sensor and an electrode, is fabricated by coating flattened and etched Pt wires with insulating, electrophoretically deposited paint. The flattened portion of the probe provides a flexible cantilever (force sensor), while the coating procedure acts to insulate the wire, such that only the tip (electrode) remains exposed to solution.[18] The etching[19] (and flattening)[20] of bare metal wires has been used previously as a procedure for the construction of tips suitable for scanning electrostatic force microscopy,[19a,b] lateral force microscopy,[19c] and conducting-AFM.[20] The SECM−AFM technique is illustrated with simultaneous topographical and electrochemical contact mode imaging studies of track-etched polycarbonate ultrafiltration membranes and topographical imaging of the surface of an ionic crystal after the SECM−AFM tip has been used to electrochemically induce dissolution from a localized region of a solid substrate.

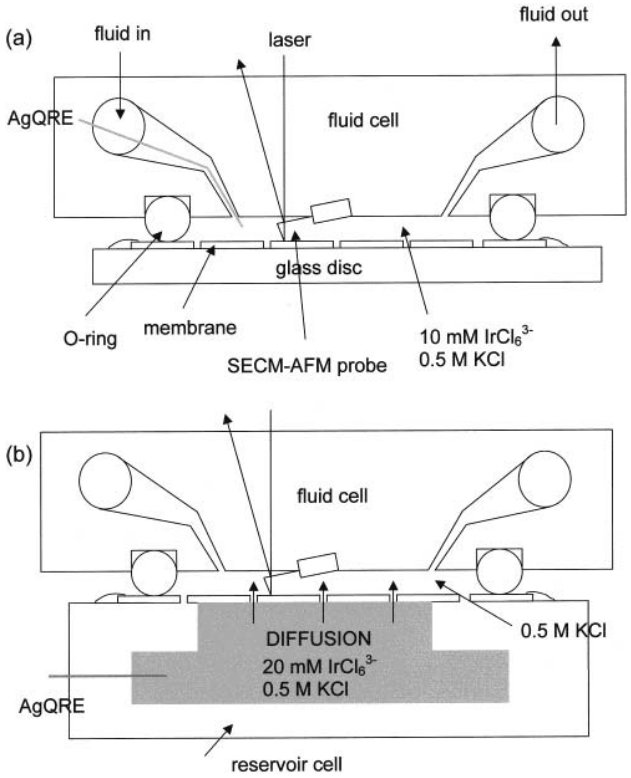


Figure 1. Schematic of the experimental setup for SECM−AFM imaging of a porous membrane under solution: (a) in the absence and (b) in the presence of an external concentration gradient.

## EXPERIMENTAL SECTION

**Materials.** All solutions were prepared from Milli-Q (Millipore Corp.) reagent water. Solutions contained potassium iridium(III) hexachloride (Sigma-Aldrich) at a concentration of either 0.01 or 0.02 mol dm$^{-3}$, in 0.5 mol dm$^{-3}$ potassium chloride (Fisons, AR grade), the latter serving as a supporting electrolyte. For dissolution imaging experiments, a 3.5 mol dm$^{-3}$ potassium chloride solution saturated with respect to potassium ferrocyanide trihydrate (Aldrich, ACS grade) was employed.

Circular samples of polycarbonate track-etched ultrafiltration membrane (Millipore) of diameter 13 mm, thickness 10 $\mu$m, and nominal pore sizes 0.6 and 1.2 $\mu$m were used as the model porous substrates. To image the membrane in an electroactive solution, the porous sample was first fixed to a glass disk, 1.2 cm in diameter, using a 1:1 mixture of nail varnish and Superglue (Bostik, Leicester, U.K.), carefully applied around the edges of the membrane. This arrangement was used as the substrate in a commercially available fluid cell (Digital Instruments, Santa Barbara, CA), as shown schematically in Figure 1a.


(14) (a) Shalom, S.; Lieberman, K.; Lewis, A.; Cohen, S. R. *Rev. Sci. Instrum.* **1992**, *63*, 4061. (b) Keller, T. H.; Rayment, T.; Klenerman, D.; Stephenson, R. J. *Rev. Sci. Instrum.* **1993**, *68*, 1448. (c) Muramatsu, H.; Chiba, N.; Homma, K.; Nakajima, K.; Ohta, S.; Kusumi, A.; Fujihira, M. *Appl. Phys. Lett.* **1995**, *66*, 3245.

(15) (a) Hansma, P. K.; Drake, B.; Marti, O.; Gould, S. A. C.; Prater, C. B. *Science* **1989**, *243*, 641. (b) Proksch, R.; Lal, R.; Hansma, P. K.; Morse, D.; Stucky, G. *Biophys. J.* **1996**, *71*, 2155. (c) Korchev, Y. E.; Bashford, C. L.; Milovanovic, M.; Vodyanoy, I.; Lab, M. J. *Biophys. J.* **1997**, *73*, 653.

(16) Macpherson, J. V.; Unwin, P. R.; Hillier, A. C.; Bard, A. J. *J. Am. Chem. Soc.* **1996**, *118*, 6445.

(17) Jones, C. E.; Macpherson, J. V.; Unwin, P. R. *Electrochem. Commun.* **1999**, *1*, 55.

(18) Slevin, C. J.; Gray, N. J.; Macpherson, J. V.; Webb, M. A.; Unwin, P. R. *Electrochem. Commun.* **1999**, *1*, 282.

(19) (a) Sørensen, A. H.; Hvid, U.; Mortensen, M. W.; Mørch, K. A. *Rev. Sci. Instrum.* **1999**, *70*, 3059. (b) Stern, J. E.; Terris, B. D.; Mamin, H. J.; Rugar, D. *Appl. Phys. Lett.* **1988**, *53*, 2717. (c) Mate, C. M.; McClelland, G. M.; Erlandsson, R.; Chang, S. *Phys. Rev. Lett.* **1987**, *59*, 1942.

(20) Peterson, C A.; Workman, R. K.; Yao, X.; Hunt, J. P.; Sarid, D. *Nanotechnology* **1998**, *9*, 331.

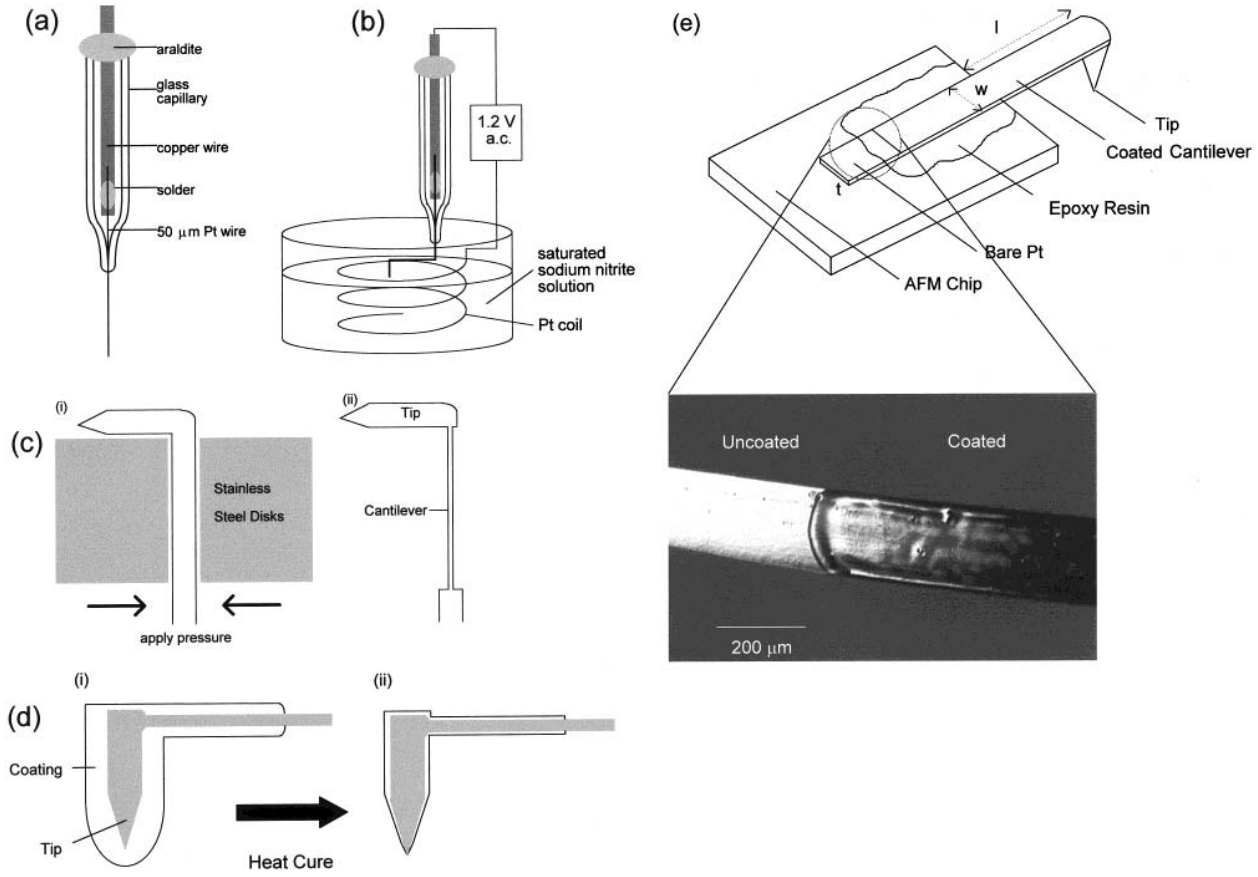


Figure 2. Schematic of the steps involved in the fabrication of SECM−AFM tips. (a) A Pt microwire electrode is constructed. (b) The Pt is etched to a fine point. (c) The cantilever component of the SECM−AFM tip is fabricated by compression. (d) The electrode and cantilever are insulated by the electrodeposition of a paint (i), which retracts from the tip end during heat curing to expose a small Pt electrode (ii). (e) The probe is affixed to the main body of an AFM using epoxy resin. Electrical contact to the SECM−AFM tip is made via the metal spring clasp of the fluid cell holder that rests on the exposed Pt section of the cantilever, which is subsequently insulated. The inset to (e) shows a micrograph of a Pt cantilever half-coated with electrodeposited paint.

For imaging diffusional transport through the membrane, a polyetheretherketone (PEEK) reservoir cell was employed,[17] which was 15 mm in diameter and 3.5 mm in height, with a rectangular opening on the top surface (1.5 mm × 2 mm) leading to an internal solution chamber (reservoir). A small hole (0.5 mm in diameter) in the top surface enabled the reservoir to be filled with the appropriate solution. Ag wire (diameter 0.125 mm) was inserted through a hole in the side of the reservoir cell and secured in place using epoxy resin (Araldite; Evode Ltd. Stafford, U.K.). This served as an Ag quasi-reference electrode (AgQRE). The reservoir (donor compartment) was filled with solution containing both supporting electrolyte and electroactive mediator. The ultrafiltration membrane was sealed over the reservoir opening using a 1:1 mixture of nail varnish and Superglue. The receptor compartment was formed by positioning the fluid cell over the underlying reservoir cell and filling with solution containing only supporting electrolyte (at the same concentration as in the reservoir). This experimental arrangement is depicted schematically in Figure 1b.

Potassium ferrocyanide trihydrate crystals were grown from seeds in saturated aqueous solution through slow evaporation. Slow growth, over 7−8 weeks, yielded well-defined monoclinic (tabular) crystals with an average length of 1 cm.[21] Experiments were carried out on the (010) surface. A glass disk, 1.2 cm in diameter, was used as the substrate for negative feedback approach curve measurements.[22]

**SECM−AFM Tip Fabrication.** The procedure for the fabrication of the SECM−AFM tips is outlined in Figure 2. First an approximate 3 cm length of 50 $\mu$m diameter hard platinum wire (Goodfellow, Cambridge, U.K.) was soldered to a solid-core tinned-copper connecting wire (RS Components, Corby, U.K.). This assembly was then mounted in a glass capillary (2.00 mm o.d., 1.16 mm i.d.; Clark Electromedical Instruments, Reading, U.K.) that had been drawn to a fine point using a pipet puller (model PB7, Narishige, Japan), such that ∼2.5 cm of the microwire protruded from the tip of the capillary. The microwire was secured in position by melting the glass tip of the capillary around the wire, using a resistively heated (20 V ac applied) Nichrome wire coil. The resulting ensemble is depicted in Figure 2a.

The end ∼0.5 mm length of the Pt microwire was bent at right angles by placing the wire on the edge of a finely polished, stainless steel block, such that the desired length was overhanging, and then pushing gently downward using the fine point of a pair of tweezers. Etching of the bent Pt microwire to form a sharp point was accomplished using a procedure adapted from Lee et

(21) Macpherson, J. V.; Unwin, P. R. *J. Phys. Chem.* **1995**, *99*, 3338.
(22) Kwak, J.; Bard, A. J. *Anal. Chem.* **1989**, *61*, 1221.

al.[18,23] (Figure 2b). The capillary was first attached to a model 9064, New Focus (Santa Clara, CA) *x*, *y*, *z* stage. The *z* (normal) axis was controlled by a micrometer (New Focus; model 9353) and the *x* and *y* axes were moved with fine adjustment screws (New Focus; model 930X). Approximately 0.3−0.4 mm of the bent length of wire was immersed in the electrochemical etch solution, which comprised saturated sodium nitrite (97% super free flowing grade, Sigma-Aldrich). An ac voltage of ∼1.2 V was applied between the microwire and a platinum coil counter electrode. To ensure symmetrical etching of the tip, the wire was placed in the center of the coil. The etching procedure was completed when the current dropped to zero, indicating that the wire was no longer in contact with the solution. The tip was then rinsed with copious amounts of deionized water.

Fabrication of the cantilever component of the SECM−AFM tip was achieved by pressing the unetched part of the microwire between two stainless steel disks (5 mm in diameter; machined from bearings) using a vice (Figure 2c). The disks had been polished to a mirror finish using a succession of polishing pads (15, 9, 6, and 1 $\mu$m diamond and 0.05 $\mu$m alumina; Buehler, Coventry, U.K.). This procedure was essential in order to prevent imperfections from the steel disks being transferred to the wire during the flattening procedure, which might result in incomplete insulator coverage, during the next stage of production.[24]

Insulation was achieved using an anodic electrodeposition paint[18,25,26] (Glassophor ZQ 84-3225, BASF, Münster, Germany). Prior to use, the anodic paint was diluted with water (1:20 by volume). A dc potential of 2 V for 3 s was applied between the SECM−AFM tip and a Pt coil in which the ensemble was centrally located. The wire was immersed in the electrodeposition paint solution, such that the tip and at least two-thirds of the cantilever were covered by the solution during the coating procedure (Figure 2di). After the wire was removed from the solution, the coating was hardened by heating at 200 °C for 3 min. Film shrinkage during heat curing of the film leaves only sharp features exposed, where the coating thins and retracts (Figure 2dii).[18] For the SECM−AFM tip, fabricated as described, only the very end of the etched tip is left exposed.

After insulation, the SECM−AFM probe was removed from the main body of the glass capillary-microwire arrangement (Figure 2a) by cutting across the exposed Pt section of the cantilever, using a sharp blade. The tip was then transferred to the underside of a commercial AFM probe (Digital Instruments), from which the tips and cantilevers had been removed, and fixed in position using epoxy resin (Figure 2e). The position of the cantilever was adjusted, such that the desired length overhung from the body of the probe. The insulating film, deposited over the cantilever, was ∼5 $\mu$m thick and observed to be smooth and transparent (Figure 2e). These were essential properties of the film, as displacements in the cantilever were measured by monitoring the deflection of a laser beam from the back of the cantilever.[27] The film layer in the vicinity of the tip was much thinner, as described later. Electrical contact to the SECM−AFM tip was made via the metal spring clasp of the commercial fluid cell holder,[16,17,28] which rested on the exposed Pt section of the cantilever. This was subsequently coated with a nail varnish/Super glue (1:1) mixture, which acted as an insulator.

Visual inspection of the SECM−AFM probes was carried out using an Olympus BH2 light microscope, equipped with a 3-CCD color video camera system (JVC, model KY-F55BE). The camera was linked to a video capture card (Image Grabber/PCI, Neotech) that allowed the images to be transferred to a PC. For higher resolution imaging, a JEOL JSM-6100 scanning electron microscope was employed.

**Instrumentation.** A Nanoscope E AFM, equipped with a 120 $\mu$m × 120 $\mu$m scanner, and fluid cell were used for SECM−AFM measurements. The instrument was placed on a Newport Corp. (Newbury, CT) SHP series subhertz platform, which in turn was placed on a custom-built granite bench incorporating vibration isolators. The AFM was shielded using a home-built Faraday cage. All images were acquired using the contact mode of operation. The tip−sample force was minimized just before imaging by reducing the set point to a value just prior to tip disengagement. AFM probes (Digital Instruments) consisted of silicon nitride cantilevers (length 200 $\mu$m, manufacturer's nominal spring constant 0.06 N m$^{-1}$) with integrated pyramidal tips, which had a height of 2.86 $\mu$m and a base width of 4 $\mu$m.

Amperometric measurements generally employed a two-electrode setup, with a silver wire (Goodfellow) operating as an AgQRE and the SECM−AFM tip functioning as the working electrode. The current was measured and the potential controlled using a model EI-400 bipotentiostat (Cypress Systems, Lawrence, KS) high-gain preamplifier, connected to a purpose-built triangular wave/pulse generator (Colburn Instruments, Coventry, U.K.). The current was recorded directly to an auxiliary output using a signal access module (Digital Instruments), allowing the simultaneous recording of electrochemical and topographical data by the AFM instrumentation.

## RESULTS AND DISCUSSION

**SECM−AFM Tip Characterization. (a) Optical and Scanning Electron Microscopy.** Figure 3a shows an optical micrograph of a representative SECM−AFM tip and cantilever fabricated using the procedure described above. The etching process typically resulted in tips 100−250 $\mu$m in length, while the flattening procedure produced cantilevers with an average width, *w*, in the range 200−250 $\mu$m and a characteristic thickness, *t*, of ∼5 $\mu$m. The length of the cantilever, *l*, was typically set somewhere between 600 and 1200 $\mu$m. For a rectangular beam geometry the spring constant, *k*, is determined by[29]

$$k = (Ew/4)(t/l)^3 \qquad (1)$$

where *E* is the modulus of elasticity. In free air, the presence of a significant end mass will modify *k*. However, given that for the imaging experiments described herein, the tip is in contact with


(23) Lee, Y. H.; Tsao, G. T.; Wankat, P. C. *Ind. Eng. Chem. Fundam.* **1978**, *17*, 59.
(24) Macpherson, J. V.. unpublished results.
(25) Bach, C. E.; Nichols, R. J.; Meyer, H.; Besenhard, J. O. *Surf. Coat.* **1994**, *67*, 139.
(26) Bach, C. E.; Nichols, R. J.; Beckman, W.; Meyer, H.; Schulte, A.; Besenhard, J. O.; Jannakoudakis, P. D. *J. Electrochem. Soc.* **1993**, *140*, 1281.
(27) Meyer, G.; Amer, N. M. *Appl. Phys. Lett.* **1988**, *53*, 1045.
(28) (a) Marsden, L. L.; Friis, E. P.; Andersen, J. E. T.; Moller, P.; Ulstrup, *J. Appl. Phys. A.* **1998**, *66*, S619. (b) Wade, T.; Garst, J. F.; Stickney, J. L. *Rev. Sci. Instrum.* **1999**, *70*, 121.
(29) Albrecht, T. R.; Akamine, S.; Carver, T. E.; Quate, C. F. *J. Vac. Sci. Technol. A* **1990**, *8*, 3386.

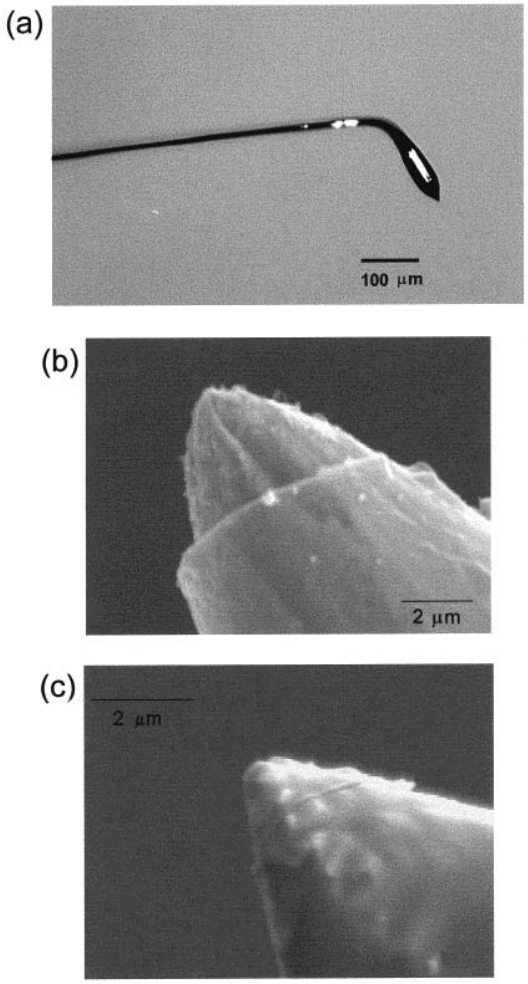


Figure 3. (a) Micrograph of a coated SECM−AFM probe. Scanning electron micrographs of the end of (b) micrometer- and (c) submicrometer-sized SECM−AFM tips.

the surface, the force constant of the probe will largely be dominated by the cantilever. Thus, eq 1 serves as a useful approximation for $k$ in imaging applications. Assuming $E = 1.7 \times 10^{10}$ N m$^{-2}$ for Pt,[30] $w = 200$ $\mu$m, $t = 5$ $\mu$m, and $l = 600-1200$ $\mu$m, eq 1 predicts $k = 0.06-0.5$ N m$^{-1}$, which is in the same range (0.06−0.58 N m$^{-1}$) as commercially available silicon nitride cantilevers with integrated tips. By doubling the length of the cantilever, from 600 to 1200 $\mu$m, it is possible to reduce the spring constant of the beam by almost 1 order of magnitude.

Parts a and b of Figure 3 respectively show typical high-resolution scanning electron micrographs of the apex of coated micrometer- and submicrometer-sized tips. The larger sized electrode was coated only once with the electrodeposition paint, while the smaller tip was coated twice. In general, it was found that increasing the number of applied depositions decreased the size of the exposed electroactive area.[18] Clearly evident, in Figure 3b, is the Pt tip and the surrounding insulator, which has covered the Pt surface with a smooth film, except in the vicinity of the tip, where the film has thinned and retracted from the apex. Although this image is useful for determining the geometry and dimensions of the exposed electrode, in practice this tip is too large for high-resolution SECM−AFM imaging. In general, electrodes with effective radii of ≤1 $\mu$m were employed, such as that shown in Figure 3c. Although it is not possible to predict the precise geometry of the exposed tip from the image in Figure 3c, electrodes fabricated from coated, etched metal wires are often approximated as being conical or hemispherical.[18,31,32]

**(b) Steady-State Voltammetry.** The exposed area of the SECM−AFM tips was estimated using linear sweep voltammetry, for the oxidation of 0.01 mol dm$^{-3}$ $IrCl_6^{3-}$, with the coated probe immersed in the electroactive solution. By measuring the steady-state diffusion-controlled current, $i(\infty)$, it is possible to determine the effective electrode radius, by assuming that the exposed tip is hemispherical.[18,31,32] Under these conditions eq 2 applies, where

$$i(\infty) = 2\pi naFDc^* \qquad (2)$$

$D$ and $c^*$ are the diffusion coefficient and concentration of the electroactive species, respectively, $n$ is the number of electrons transferred per redox event, $F$ is Faraday's constant, and $a$ is the radius of the exposed tip. Figure 4a shows a typical voltammetric response, recorded at a potential scan rate of 10 mV s$^{-1}$ for an SECM−AFM tip. Two applications of insulating paint were applied to this particular probe. The current−voltage characteristics on a given probe were found to be reproducible over a period of several days.[18] Assuming a hemispherical geometry and $D_{IrCl_6^{3-}} = 7.5 \times 10^{-6}$ cm$^2$ s$^{-1}$,[33] $i(\infty) = 0.80$ nA indicates an effective tip radius of ∼180 nm (eq 2). In general, for the range of SECM−AFM probes tested voltammetrically (over 50 were investigated in total), effective tip radii in the range 0.05−2.5 $\mu$m were determined.

**(c) Approach Curve Measurements.** Although at the simplest level the tip electrode can be approximated as hemispherical, SEM images often show that this can oversimplify the true geometry; for example, the exposed tip in Figure 3b appears more cone-shaped than hemispherical. Given that the steady-state diffusion-limited current, measured as a function of the tip−substrate separation, is sensitive to the geometry of the electrode,[22,34−36] for both insulating and conducting substrates, approach (and retract) curves provide more detailed information on the shape of a tip. Parts a and b of Figure 4 respectively show typical probe deflection and limiting current data, recorded simultaneously, for the oxidation of 0.01 mol dm$^{-3}$ $IrCl_6^{3-}$, as a function of the distance, $d$, between the tip (the voltammetric response of which is shown in Figure 4a) and an inert glass substrate. The substrate was translated toward and away from the electrode, biased at +1.0 V versus AgQRE, at a scan speed of 0.2 $\mu$m s$^{-1}$.

As the inert substrate approaches the tip, the limiting current decreases (Figure 4c) as diffusion of electroactive species to the electrode becomes more hindered,[22,35] ultimately resulting in a

(30) Kaye, G. W. C.; Laby, T. H. *Tables of Physical and Chemical Constants*; Longman: Harlow, U.K., 1995; p 44.

(31) Penner, R. M.; Heben, M. J.; Longin, T. L.; Lewis, N. S. *Science* **1990**, *250*, 1118.

(32) Penner, R. M.; Heben, M. J.; Lewis, N. S. *Anal. Chem.* **1989**, *61*, 1630.

(33) Macpherson, J. V.; Jones, C. E.; Unwin, P. R. *J. Phys. Chem. B* **1998**, *102*, 9891.

(34) Davis, J. M.; Fan, F.-R. F.; Bard, A. J. *J. Electroanal. Chem.* **1987**, *238*, 1.

(35) Mirkin, M. V.; Fan, F.-R. F.; Bard, A. J. *J. Electroanal. Chem.* **1992**, *328*, 47.

(36) Shao, Y.; Mirkin, M. V.; Fish, G.; Kokotov, S.; Palanker, D.; Lewis, A. *Anal. Chem.* **1997**, *69*, 1627.

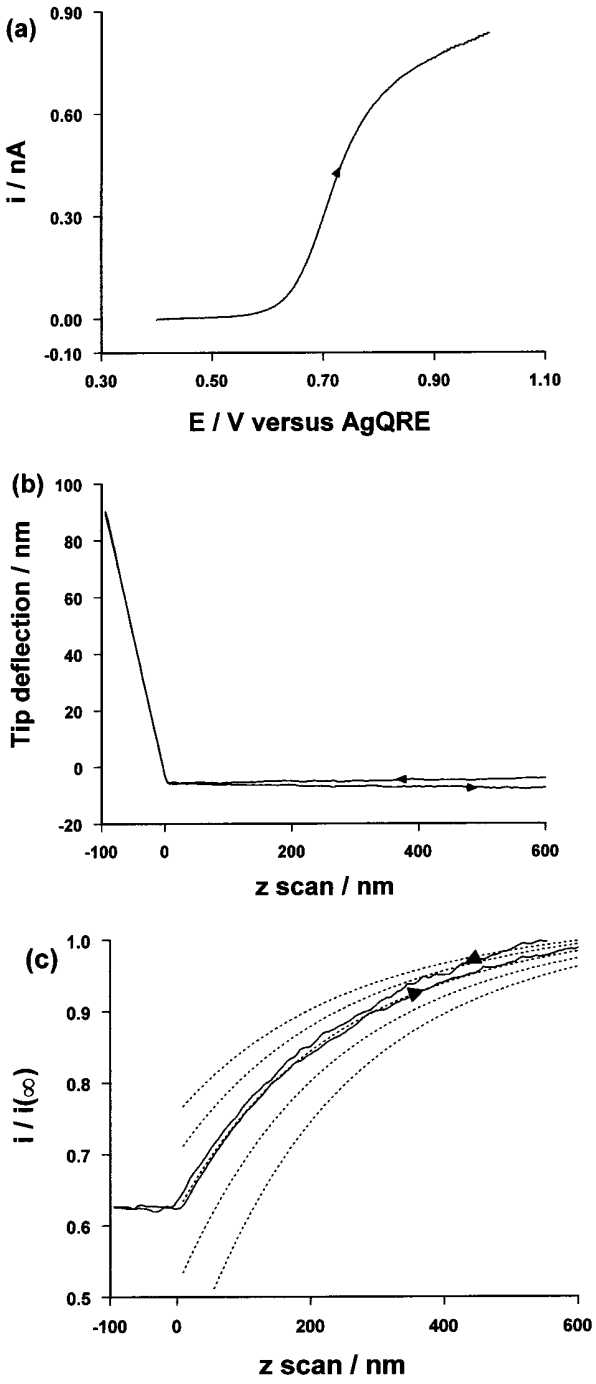


Figure 4. (a) Steady-state voltammogram recorded at 10 mV $s^{-1}$ for the oxidation of 0.01 mol $dm^{-3}$ $IrCl_6^{3-}$ in 0.5 mol $dm^{-3}$ KCl, at an SECM−AFM tip with an effective radius of 180 nm, calculated using eq 2. Simultaneously recorded cantilever deflection (b) and the diffusion-controlled limiting current (c) for the oxidation of 0.01 mol $dm^{-3}$ $IrCl_6^{3-}$ in 0.5 mol $dm^{-3}$ KCl, as a function of the SECM−AFM tip separation from an inert glass substrate. The surface was scanned toward and away from the tip, biased at +1.0 V versus AgQRE, at a scan speed of 0.2 $\mu$m $s^{-1}$. The theory lines (···) correspond to *b* values of 1.0 (lower curve), 1.5, 2.0, 2.5, and 3.0 (upper curve).

plateau when the tip is in contact with the surface. The contact point determined electrochemically (Figure 4c) agrees well with that determined from the deflection characteristics of the probe (Figure 4b). The position at which the cantilever suddenly begins to deflect (indicating the onset of constant compliance for this particular hard surface) can be taken unambiguously as the point of contact between the tip and the substrate.[37] Repeated approach and retract curves, recorded after acquisition of the results displayed in Figure 4b and c, resulted in very similar responses, indicating that the overall electrode geometry had not been significantly altered upon contact with the glass substrate. This is not unexpected with the SECM−AFM probes employed, because as the surface contacts and begins to push against the tip, it is the cantilever, and not the tip, that will deflect. This is an attractive feature of the technique, as it prevents tip damage if the electrode is forced significantly past the point of contact with the underlying surface.

To fit the experimental data to the theoretical current−distance response, assuming a conical tip geometry, three parameters are required: the radius of the cone, *r*, the height of the cone, *h*, to provide

$$b = h/r \tag{3}$$

and the tip−substrate contact point.[35] Previous SECM approach curve measurements performed to characterize small tip geometries have either made an arbitrary adjustment of the $i/i(\infty) - d$ curve to fit the theoretical response[35] or employed time-of-flight measurements,[38] to estimate the tip−substrate separation,[36] prior to the approach curve measurement. For the SECM−AFM probes employed here, such procedures are unnecessary as the tip−substrate contact point can be obtained unequivocally from cantilever deflection−distance approach curves. The theoretical $i/i(\infty) - d$ response for a range of different cone geometries, characterized by *b* values of 1.0 (lower curve), 1.5, 2.0, 2.5, and 3.0 (upper curve), are also shown in Figure 4c. The experimental data were found to be best described by a *b* value of 2.0 and an *r* value of 190 nm. The data did not conform to the theory for a hemispherical tip.

**SECM−AFM Imaging of Porous Membranes. (a) Hindered Diffusion.** Parts a and b of Figure 5 show, respectively, the height and current images of a track-etched membrane, recorded simultaneously with an SECM−AFM tip, characterized by an effective hemispherical radius, $a = 1.1$ $\mu$m, of a dimension similar to the pore. The scan size is $50 \times 50$ $\mu$m (comprising 256 lines), imaged at a scan rate of 25 $\mu$m $s^{-1}$. The tip was scanned from left to right (fast scan axis) and top to bottom (slow scan axis). The membrane was fully immersed in a solution containing 0.01 mol $dm^{-3}$ $IrCl_6^{3-}$ and 0.5 mol $dm^{-3}$ KCl. The tip was held at a potential of +1.0 V versus AgQRE, sufficient to electrolyze the solution mediator at a diffusion-controlled rate.

Figure 5a clearly demonstrates the ability of the SECM−AFM probe to resolve the topography of the membrane surface. The size of the pore diameters measured from this image—1.5 ± 0.3 $\mu$m—closely correlates with those determined by conventional AFM, employing a standard silicon nitride probe in contact mode. The slight elongation of the pores in the direction of the slow scan axis arises possibly from the sharp tip getting caught within

(37) Weisenhorn, A. L.; Khorsandi, M.; Kasas, S.; Gotzos, V.; Butt, H.-J. *Nanotechnology* **1993**, *4*, 106.

(38) (a) Feldman, B. J.; Feldberg, S. W.; Murray, R W. *J. Phys. Chem.* **1987**, *91*, 6558. (b) Mirkin, M. V.; Arca, M.; Bard, A. J. *J. Phys. Chem.* **1993**, *97*, 10790.

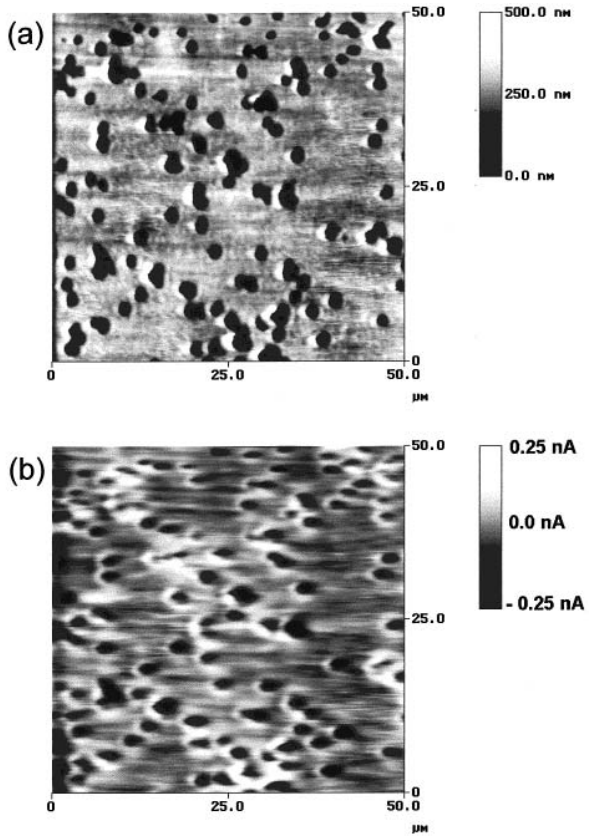


Figure 5. Simultaneously recorded (a) height and (b) current ($\Delta i$) images of a track-etched membrane, obtained with an SECM−AFM tip, characterized by an effective tip radius, $a = 1.1$ $\mu$m. The scan size was 50 × 50 $\mu$m, imaged at a scan rate of 25 $\mu$m s$^{-1}$, with $i_{mean} \approx 2.9$ nA. The tip was scanned from left to right (fast scan axis) and top to bottom (slow scan axis). The membrane was fully immersed in a solution containing 0.01 mol dm$^{-3}$ $IrCl_6^{3-}$ and 0.5 mol dm$^{-3}$ KCl. The tip was held at a potential of +1.0 V versus AgQRE, sufficient to electrolyze the solution mediator at a diffusion-controlled rate.

the pores during imaging. The random grouping and overlap of many of the pores is a real effect, also observed with SEM. To emphasize the variations in the electrochemical current data, the image in Figure 5b has been zero-order flattened,[39] a process that involves subtracting the mean current value, $i_{mean}$, for the whole image from the measured current, $i_{measure}$, recorded at every pixel in the image, to give

$$\Delta i = i_{measure} - i_{mean} \quad (4)$$

As Figure 5b clearly shows, there is a decrease in the measured limiting tip current associated with each pore.

With the tip in contact with the membrane, away from a pore, the diffusion profile of electroactive mediator to the electrode is as depicted in Figure 6i. Species can diffuse around the sides of the electrode, but are hindered in the contact region of the tip with the surface. With the tip inside the pore, the situation is most likely as shown in Figure 6ii. Under these conditions, hemispherical diffusion of electroactive species to the tip will be hindered

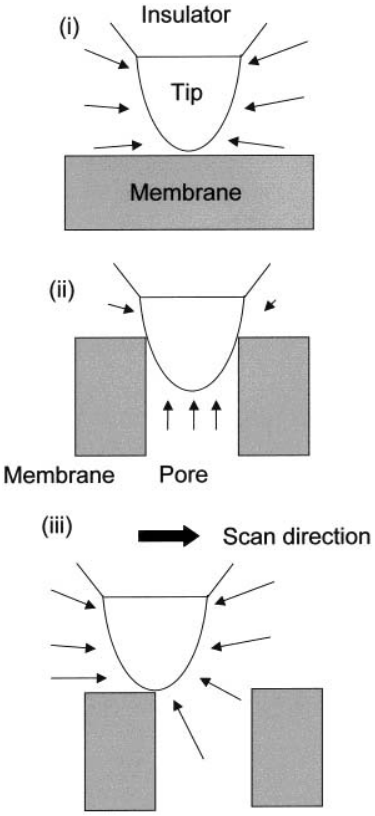


Figure 6. Schematic of the diffusion profiles established at a conically shaped electrode, with the tip (of similar size to the pore) (i) in contact with the membrane, far from a pore, (ii) in the pore, and (iii) on the leading edge of the pore.

by the walls of the pore, resulting in a predominantly linear diffusion profile at the end of the tip. The current imaging results suggest diffusional restriction is more extensive in the membrane pores than with the tip on the surrounding planar areas of the membrane.

Figure 5b also shows that, for the majority of pores, the diffusion-limited current appears to be greater on the left-hand edge compared to the right-hand edge. The general current increase at the leading edge is a consequence of enhanced diffusion at the tip, as shown schematically in Figure 6iii. The decrease in current at the trailing edge is thought to be due to depletion within the pore, arising in response to the tip scan speed, $v_{scan}$, employed. The *maximum* residence time, $t_{res}$, of the tip in the vicinity of the pore is estimated as

$$t_{res} = d_{pore}/v_{scan} \quad (5)$$

where $d_{pore}$ is the diameter of the pore. This yields $t_{res} \approx 0.06$ s, for $d_{pore} = 1.5$ $\mu$m. This suggests a *maximum* diffusion layer thickness, $\delta$, in the pore, based on Cottrellian behavior[40]

$$\delta = \sqrt{D\pi t_{res}} \quad (6)$$

of up to 12 $\mu$m, assuming $D = 7.5 \times 10^{-6}$ cm$^2$ s$^{-1}$. Thus, as the tip scans over the hole, depletion effects inside the pore are likely

(39) Digital Instruments. *Command Reference Manual*, Version 4.20; 1996; Chapter 13, p 15.

(40) Brett, C. M. A.; Brett, A. M. O. *Electrochemistry, Principles, Methods and Applications*; Oxford University Press: Oxford, U.K., 1996; p 95.

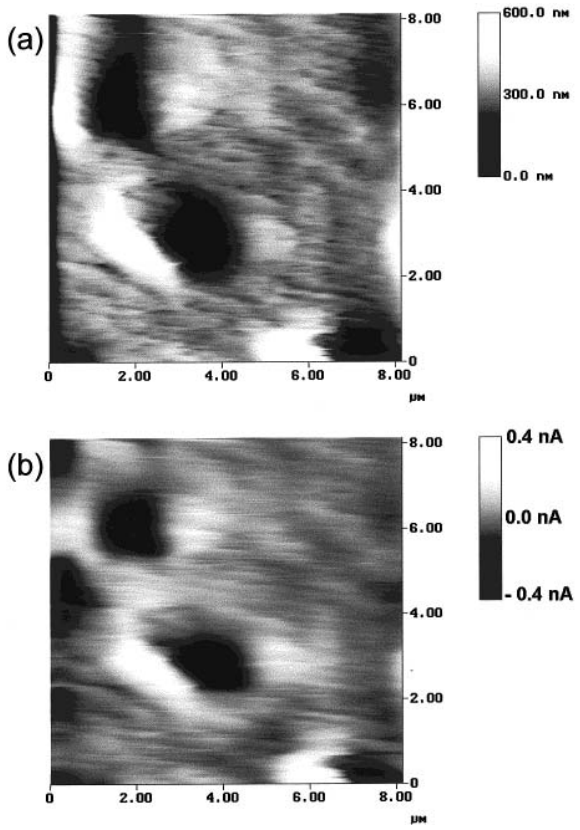


Figure 7. Simultaneous (a) height and (b) current ($\Delta i$) images of the track-etched membrane, obtained with the same SECM−AFM tip as for Figure 5. The scan size is 8 × 8 $\mu$m, imaged at a scan rate of 4 $\mu$m s$^{-1}$, with $i_{mean} \approx 3.8$ nA. The tip was scanned from left to right (fast scan axis) and top to bottom (slow scan axis).

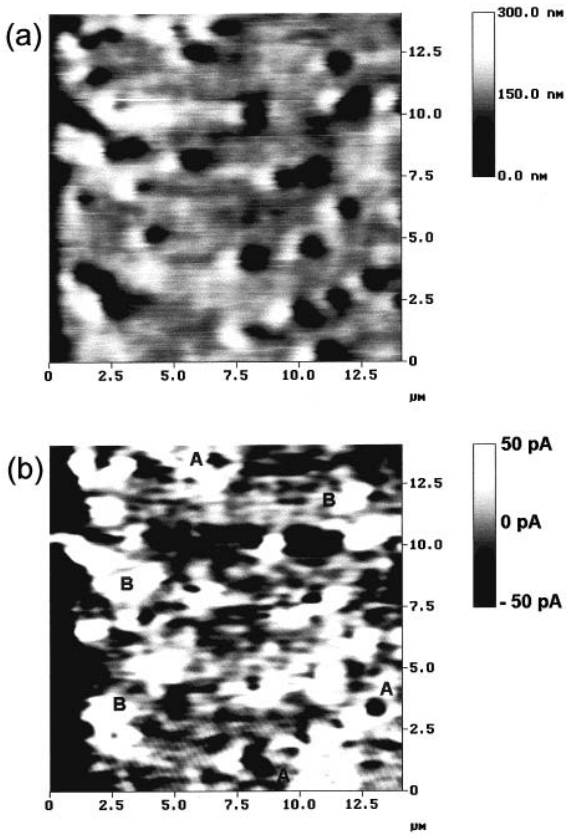


Figure 8. Simultaneous (a) height and (b) current ($\Delta i$) images of a track-etched membrane, obtained with an SECM−AFM tip, characterized by an effective conical tip radius, $r = 275$ nm and $b = 2.0$. The scan size is 14 × 14 $\mu$m, and a scan rate of 7 $\mu$m s$^{-1}$ was employed, with $i_{mean} \approx 0.9$ nA. The tip was scanned from left to right (fast scan axis) and bottom to top (slow scan axis). The membrane was part of a two-compartment diffusion cell, separating the donor phase, containing 0.02 mol dm$^{-3}$ $IrCl_6^{3-}$ and 0.5 mol dm$^{-3}$ KCl, from the receptor phase, consisting of 0.5 mol dm$^{-3}$ KCl only. The tip was held at a potential of +1.0 V versus AgQRE, sufficient to electrolyze the solution mediator ($IrCl_6^{3-}$) at a diffusion-controlled rate.

to be significant, resulting in diminished diffusion to the tip when it emerges at the trailing edge of the pore compared with the situation at the leading edge, where it sees fresh solution from within the pore (Figure 6iii). In this situation, it is important to note the direction of the tip along the fast scan axis, when interpreting the current image.

Parts a and b of Figure 7 show, respectively, height and current ($\Delta i$) images of the track-etched membrane, at higher resolution, obtained with the same SECM−AFM tip used for Figure 5. The scan size is 8 × 8 $\mu$m, imaged at a scan rate of 4 $\mu$m s$^{-1}$. The tip was scanned from left to right (fast scan axis) and top to bottom (slow scan axis). Once again, the correlation between the position of a hole and a decrease in the diffusion-limited tip current is observed. The $\Delta i$ values are greater than those for Figure 5b, an effect most likely due to the slower tip scan speed employed, resulting in more pronounced depletion effects within the pore.

**(b) Imaging Diffusional Transport.** Parts a and b of Figure 8 show height and current ($\Delta i$) images, respectively, of a track-etched membrane, obtained with a tip, characterized by an effective conical tip radius, $r = 275$ nm and $b = 2.0$ (using approach curve measurements, as described above). The scan size is 14 × 14 $\mu$m, and a scan rate of 7 $\mu$m s$^{-1}$ was employed. The tip was scanned from left to right (fast scan axis) and bottom to top (slow scan axis). The membrane was part of a two-compartment reservoir cell (Figure 1b), separating a donor phase, containing 0.02 mol dm$^{-3}$ $IrCl_6^{3-}$ and 0.5 mol dm$^{-3}$ KCl, from the receptor phase (containing the probe), consisting of 0.5 mol dm$^{-3}$ KCl only. The tip potential was +1.0 V versus AgQRE, sufficient to electrolyze the solution mediator ($IrCl_6^{3-}$) at a diffusion-controlled rate. Just prior to imaging, fresh 0.5 mol dm$^{-3}$ KCl solution was flushed through the receptor compartment.

Cross-sectional height analysis of the data in Figure 8a reveals a mean pore diameter of 0.7 ± 0.1 $\mu$m, consistent with conventional AFM measurements. The current image in Figure 8b represents the highest resolution SECM map of ion transport pathways through a porous membrane and—in conjunction with Figure 8a—provides a direct correlation between surface topography and diffusional activity at the submicrometer level. These results contrast with previous SECM studies[41,42,43] using larger scale UMEs, which imaged transport activity *only* (without identifying pore structure) through porous materials.

(41) Nugues, S.; Denuault, G. *J. Electroanal. Chem.* **1996**, *408*, 125.
(42) (a) Macpherson, J. V.; Beeston, M. A.; Unwin, P. R.; Hughes, N. P.; Littlewood, D. *Langmuir* **1995**, *11*, 3959. (b) Macpherson, J. V.; Beeston, M. A.; Unwin, P. R.; Hughes, N. P.; Littlewood, D. *J. Chem. Soc., Faraday Trans.* **1995**, *91*, 1407.

Figure 8b indicates a marked heterogeneity in the measured current associated with different pores, with some showing small currents (label A; Figure 8b) while others show a pronounced current (label B; Figure 8b). The varying currents might be due differences in the size of the pores—for the larger sized pores, the effectiveness of the electrode in detecting diffusion out of the pore is more likely to be counterbalanced by the presence of the probe in the pore restricting diffusion out of the hole. However, direct comparison of Figure 8a and b revealed no significant correlation between pore diameter and the current measured. Thus, it is more likely that the current heterogeneities are due to actual variations in diffusional activity through the different pores. Previous SECM studies of diffusion through Nucleopore membranes with 10 $\mu$m diameter pores have hinted at this,[41] in that only a small number of enhanced-current regions were observed compared to the density of pores. The SECM−AFM clearly represents a step forward in being able to locate and investigate individual pores simultaneously and also probe pores that are up to 20 times smaller. Work is currently in progress to minimize tip diffusional hindrance contributions to the current map, by scanning the probe at a constant height above the surface, during imaging.

**Probing Dissolution.** Prior to dissolution initiation, the current−voltage response (Figure 9a) of the tip, characterized by an effective conical tip radius, $r$ = 275 nm and $b$ = 2.0, was recorded for the oxidation of $Fe(CN)_6^{4-}$ in a solution containing saturated potassium ferrocyanide trihydrate and 3.5 mol dm$^{-3}$ potassium chloride. For this measurement, the probe was positioned far from the surface of the crystal in the bulk of the solution. The topography of the surface was then imaged and an area of the surface that was largely featureless, containing only one main terraced region, selected. With the tip positioned in the center of the scan (by reducing the scan size to 0 nm × 0 nm) and in contact with the surface, the electrode potential was pulsed from open circuit to a value sufficient to oxidize the saturated concentration of lattice ions in solution ($Fe(CN)_6^{4-}$) at a diffusion-controlled rate (+0.7 V versus AgQRE: see Figure 9a) for a time period of ∼10 s. The potential was then returned to open circuit. This process serves to create an undersaturation at the crystal/solution interface which drives the dissolution process,[16,21,44] as shown schematically in Figure 9b.

Figure 9c shows a height image of the (010) surface of a potassium ferrocyanide trihydrate single crystal, recorded immediately after the SECM−AFM probe had been used to electrochemically induce dissolution. For this image, a tip scan rate of 41 $\mu$m s$^{-1}$ was employed. The presence of an electrochemically induced macroscopic etch pit in the center of the scan image is evident. The bottom of the dissolution feature is unresolvable, as the depth exceeds the $z$ travel of the piezopositioner. The areas directly surrounding the pit are predominantly planar, separated by steps varying from nanometer to tens of nanometers in height.

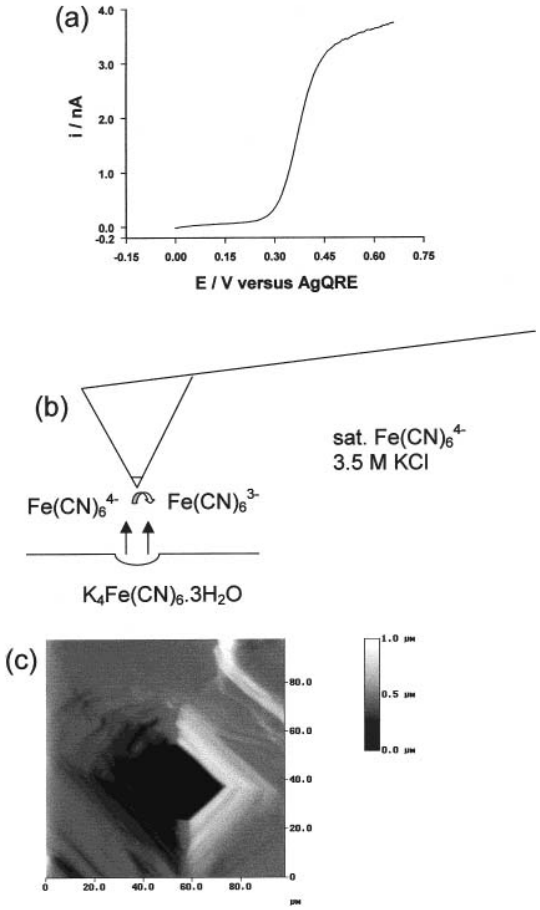


Figure 9. (a) Steady-state voltammogram recorded at 10 mV s$^{-1}$ for the oxidation of $Fe(CN)_6^{4-}$ at an SECM−AFM tip in a solution containing saturated potassium ferrocyanide trihydrate and 3.5 mol dm$^{-3}$ potassium chloride. The tip electrode was characterized by an effective conical tip radius, $r$ = 275 nm and $b$ = 2.0. (b) Schematic of the principles involved in SECM−AFM induced dissolution of a localized zone on a single crystal of potassium ferrocyanide trihydrate. (c) SECM−AFM height image of the (010) surface of a potassium ferrocyanide trihydrate single crystal in a solution containing saturated potassium ferrocyanide trihydrate and 3.5 mol dm$^{-3}$ KCl, recorded immediately after the tip electrode had been used to electrochemically induce dissolution, with the tip positioned in the center of the scan. For this image, a tip scan rate of 41 $\mu$m s$^{-1}$ was employed.

The large dimensions of the etch pit are not surprising in light of earlier SECM investigations on the dissolution kinetics of the (010) surface of potassium ferrocyanide trihydrate,[21] which showed that the dissolution process is extremely fast.

The image in Figure 9c highlights one of the powerful attributes of SECM−AFM: the possibility of making very high spatial electrochemical and topographical measurements with a single probe. Although SECM, in isolation, can provide valuable quantitative information on local dissolution rates, important complementary topographical information has, in the past, been limited to microscopic studies of reacted surfaces at a resolution only on the micrometer scale, either ex situ using optical microscopy[21,44c,d] or in situ employing the SECM negative feedback mode,[21] with an additional solution mediator. Further studies, using this methodology to target a region for subsequent electrochemical investigation, are currently in progress.


(43) (a) Bath, B. D.; Lee, R. D.; White, H. S. *Anal. Chem.* **1998**, *70*, 1047. (b) Lee, R. D.; White, H. S.; Scott, E. R. *J. Pharm. Sci.* **1995**, *85*, 1186. (c) Scott, E. R.; Phipps, J. B.; White, H. S. *J. Invest. Dermatol.* **1995**, *104*, 142. (d) Scott, E. R.; Laplaza, A. I.; White, H. S.; Phipps, J. B. *Pharm. Res.* **1993**, *10*, 1699. (e) Scott, E. R.; White, H. S.; Phipps, J. B. *Anal. Chem.* **1993**, *65*, 1537.

(44) (a) Macpherson, J. V.; Unwin, P. R. *J. Phys. Chem.* **1996**, *100*, 19475. (b) Macpherson, J. V.; Unwin, P. R. *J. Phys. Chem.* **1995**, *99*, 14824. (c) Macpherson, J. V.; Unwin, P. R. *J. Phys. Chem.* **1994**, *98*, 3109. (d) Macpherson, J. V.; Unwin, P. R. *J. Phys. Chem.* **1994**, *98*, 1704.

## CONCLUSIONS

The development of a combined SECM−AFM represents a significant advance in SPM methodology. The probe, consisting of a flattened and etched Pt wire, electrically insulated at all but the apex of the tip, has dual electrochemical and force sensing capabilities. The instrument is thus capable of recording independent submicrometer electrochemical information simultaneously with surface topography measurements, at high resolution, under aqueous solution. There is considerable scope for using this instrument in a variety of ways to probe a whole range of substrates. For example, the chemistry or reactivity of a targeted structural feature, identified by topographical mapping, could be investigated using electrochemistry; or topographical and structural changes of a substrate could be mapped in response to a local chemical perturbation. In order examine a more diverse range of systems, we plan to use a noncontact mode version of this technique, which will involve scanning the tip over the surface, first in contact mode, to record substrate topography (by monitoring the deflection of the cantilever) and then, with the tip retracted a known distance from the sample, to record the electrochemical response of the tip electrode. This approach would enable us to look at conducting and semiconducting surfaces as well as the insulating substrates of interest here.

The capabilities of SECM−AFM have been illustrated with simultaneous electrochemical and topographical images of a porous membrane under solution: (a) in the absence and (b) in the presence of an external concentration gradient. In both cases, the tip was able to spatially resolve individual pores. In the former case, the probe current was found to decrease as the tip entered a pore, an effect arising from the perturbation of the diffusion field associated with the probe. In the latter studies, an increase in the current was observed over many holes, as the tip probed the diffusional flux of electroactive species emerging from the pores, an effect found to be spatially heterogeneous. To probe diffusion across the membrane, future work will investigate imaging with the tip held at a constant height above the surface.

The SECM−AFM has also proved effective at electrochemically inducing dissolution from a highly localized zone on the surface of an ionic crystal while monitoring the topographical surface change in response to this perturbation, under conditions of high spatial resolution.

## ACKNOWLEDGMENT

We appreciate support from the EPSRC (ROPA:GR/L71377). We thank Claire Jones, Dr. Chris Slevin (Department of Chemistry, University of Warwick), and Dr. Chris McConville (Department of Physics, University of Warwick) for much helpful advice and Prof. Henry White (Department of Chemistry, University of Utah) for interesting comments on the diffusion studies. We are grateful to Ken Westwood and Lee Butcher (Mechanical Workshops, Department of Chemistry, University of Warwick) for advice on the fabrication of SECM−AFM probes and for constructing the reservoir cells.

Received for review August 12, 1999. Accepted November 9, 1999.

AC990921W